

Directed Flow in 158 A·GeV $^{208}\text{Pb} + ^{208}\text{Pb}$ Collisions.

M.M. Aggarwal,¹ A. Agnihotri,² Z. Ahammed,³ A.L.S. Angelis,⁴ V. Antonenko,⁵ V. Arefiev,⁶ V. Astakhov,⁶ V. Avdeitchikov,⁶ T.C. Awes,⁷ P.V.K.S. Baba,⁸ S.K. Badyal,⁸ A. Baldine,⁶ L. Barabach,⁶ C. Barlag,⁹ S. Bathe,⁹ B. Batiounia,⁶ T. Bernier,¹⁰ K.B. Bhalla,² V.S. Bhatia,¹ C. Blume,⁹ R. Bock,¹¹ E.-M. Bohne,⁹ Z. Bőröcz,⁹ D. Bucher,⁹ A. Buijs,¹² H. Büsching,⁹ L. Carlen,¹³ V. Chalyshov,⁶ S. Chattopadhyay,³ R. Cherbachev,⁵ T. Chujo,¹⁴ A. Claussen,⁹ A.C. Das,³ M.P. Decowski,¹⁸ V. Djordjadze,⁶ P. Donni,⁴ I. Doubovik,⁵ M.R. Dutta Majumdar,³ K. El Chenawi,¹³ S. Eliseev,¹⁵ K. Enosawa,¹⁴ P. Foka,⁴ S. Fokin,⁵ V. Frolov,⁶ M.S. Ganti,³ S. Garpman,¹³ O. Gavrishchuk,⁶ F.J.M. Geurts,¹² T.K. Ghosh,¹⁶ R. Glasow,⁹ S. K.Gupta,² B. Guskov,⁶ H. Å.Gustafsson,¹³ H. H.Gutbrod,¹⁰ R. Higurashi,¹⁴ I. Hrivnacova,¹⁵ M. Ippolitov,⁵ H. Kalechofsky,⁴ R. Kamermans,¹² K.-H. Kampert,⁹ K. Karadjev,⁵ K. Karpio,¹⁷ S. Kato,¹⁴ S. Kees,⁹ H. Kim,⁷ B. W. Kolb,¹¹ I. Kosarev,⁶ I. Koutcheryaev,⁵ T. Krümpel,⁹ A. Kugler,¹⁵ P. Kulinich,¹⁸ M. Kurata,¹⁴ K. Kurita,¹⁴ N. Kuzmin,⁶ I. Langbein,¹¹ A. Lebedev,⁵ Y.Y. Lee,¹¹ H. Löhner,¹⁶ L. Luquin,¹⁰ D.P. Mahapatra,¹⁹ V. Manko,⁵ M. Martin,⁴ A. Maximov,⁶ R. Mehdiyev,⁶ G. Mgebrichvili,⁵ Y. Miake,¹⁴ D. Mikhalev,⁶ G.C. Mishra,¹⁹ Y. Miyamoto,¹⁴ D. Morrison,²⁰ D. S. Mukhopadhyay,³ V. Myalkovski,⁶ H. Naef,⁴ B. K. Nandi,¹⁹ S. K. Nayak,¹⁰ T. K. Nayak,³ S. Neumaier,¹¹ A. Nianine,⁵ V. Nikitine,⁶ S. Nikolaev,⁵ P. Nilsson,¹³ S. Nishimura,¹⁴ P. Nomokonov,⁶ J. Nystrand,¹³ F.E. Obenshain,²⁰ A. Oskarsson,¹³ I. Otterlund,¹³ M. Pachr,¹⁵ A. Parfenov,⁶ S. Pavliouk,⁶ T. Peitzmann,⁹ V. Petracek,¹⁵ F. Plasil,⁷ W. Pinanaud,¹⁰ M.L. Purschke,¹¹ B. Raeven,¹² J. Rak,¹⁵ R. Raniwala,² S. Raniwala,² V.S. Ramamurthy,¹⁹ N.K. Rao,⁸ F. Retiere,¹⁰ K. Reygers,⁹ G. Roland,¹⁸ L. Rosselet,⁴ I. Roufanov,⁶ C. Roy,¹⁰ J.M. Rubio,⁴ H. Sako,¹⁴ S.S. Sambyal,⁸ R. Santo,⁹ S. Sato,¹⁴ H. Schlagheck,⁹ H.-R. Schmidt,¹¹ G. Shabratova,⁶ I. Sibiriak,⁵ T. Siemiarczuk,¹⁷ D. Silvermyr,¹³ B.C. Sinha,³ N. Slavine,⁶ K. Söderström,¹³ N. Solomey,⁴ S.P. Sørensen,²⁰ P. Stankus,⁷ G. Stefanek,¹⁷ P. Steinberg,¹⁸ E. Stenlund,¹³ D. Stüken,⁹ M. Sumbera,¹⁵ T. Svensson,¹³ M.D. Trivedi,³ A. Tsvetkov,⁵ C. Twenhöfel,¹² L. Tykarski,¹⁷ J. Urbahn,¹¹ N.v. Eijndhoven,¹² G.J.v. Nieuwenhuizen,¹⁸ A. Vinogradov,⁵ Y.P. Viyogi,³ A. Vodopianov,⁶ S. Vörös,⁴ B. Wyslouch,¹⁸ K. Yagi,¹⁴ Y. Yokota,¹⁴ G.R. Young⁷

(WA98 Collaboration)

- ¹ University of Panjab, Chandigarh 160014, India
- ² University of Rajasthan, Jaipur 302004, Rajasthan, India
- ³ Variable Energy Cyclotron Centre, Calcutta 700 064, India
- ⁴ University of Geneva, CH-1211 Geneva 4, Switzerland
- ⁵ RRC Kurchatov Institute, RU-123182 Moscow, Russia
- ⁶ Joint Institute for Nuclear Research, RU-141980 Dubna, Russia
- ⁷ Oak Ridge National Laboratory, Oak Ridge, Tennessee 37831-6372, USA
- ⁸ University of Jammu, Jammu 180001, India
- ⁹ University of Münster, D-48149 Münster, Germany
- ¹⁰ SUBATECH, Ecole des Mines, Nantes, France
- ¹¹ Gesellschaft für Schwerionenforschung (GSI), D-64220 Darmstadt, Germany
- ¹² Universiteit Utrecht/NIKHEF, NL-3508 TA Utrecht, The Netherlands
- ¹³ Lund University, SE-221 00 Lund, Sweden
- ¹⁴ University of Tsukuba, Ibaraki 305, Japan
- ¹⁵ Nuclear Physics Institute, CZ-250 68 Rez, Czech Rep.
- ¹⁶ KVI, University of Groningen, NL-9747 AA Groningen, The Netherlands
- ¹⁷ Institute for Nuclear Studies, 00-681 Warsaw, Poland
- ¹⁸ MIT Cambridge, MA 02139, USA
- ¹⁹ Institute of Physics, 751-005 Bhubaneswar, India
- ²⁰ University of Tennessee, Knoxville, Tennessee 37966, USA

(January 17, 2014)

The directed flow of protons and π^+ have been studied in 158 A GeV $^{208}\text{Pb} + ^{208}\text{Pb}$ collisions. A directed flow analysis of the rapidity dependence of the average transverse momentum projected onto the reaction plane is presented for semi-central collisions with impact parameters ≈ 8 fm, where the flow effect is largest. The magnitude of the directed flow is found to be significantly smaller than observed at AGS energies and than RQMD model predictions.

25.75.-q,25.75.Ld,25.75.Dw

Collective flow has been studied in heavy ion collisions since first observed at the Bevalac by the Plastic Ball experiment [1]. At Bevalac energies of a few GeV per nucleon and lower, the study of collective flow has been of interest largely due to its expected sensitivity to the nuclear equation of state (EOS) [2]. However, the extraction of information on the EOS in heavy ion collisions is complicated by uncertainties in the initial dynamics of the pre-hydrodynamic stage, such as due to the momentum-dependence of the repulsive nucleon-nucleus interaction [3] and possible in-medium modifications of the nucleon-nucleon cross section [4]. Nevertheless, the importance of collective flow measurements in ultra-relativistic heavy ion collisions has been emphasized by several authors [5–9]. Collective flow development follows the time evolution of pressure gradients in the hot, dense matter. Thus, collective flow can serve as a hadronic “penetrating probe” to provide information on the initial state. In particular, the formation of a Quark Gluon Plasma (QGP) during the early stages of the collision is expected to result in reduced pressure gradients due to a softening of the EOS, with a corresponding reduction of collective flow [5,7,8].

Transverse collective flow is normally discussed in terms of its lowest order symmetries with respect to the reaction plane, which have recently been formulated in terms of a Fourier decomposition [10,11]. The lowest order component is radial flow which is characterized by an isotropic transverse flow velocity. The next component is the directed flow which is characterized by the net displacement of the flow into a particular transverse direction. The elliptic flow component corresponds to the second order Fourier coefficient of the flow pattern.

Recently, collective flow has been observed at the AGS energy of 11 A GeV [12]. The directed flow is observed to be smaller than at lower incident energy but similarly consistent with model calculations [13]. It is also observed that the elliptic flow has changed from an out-of-plane squeeze-out direction to an in-plane direction [13]. At CERN SPS energies it has recently been shown that it is possible to determine the event-plane in the target fragmentation region for ^{16}O - and ^{32}S -induced reactions [14] and also in the mid-rapidity region for ^{32}S - [15] and ^{208}Pb -induced reactions [16]. Directed flow results at SPS energies were first reported in [17] and both directed and elliptic flow results have recently been published [18]. In this letter we analyze the centrality dependence of the directed flow of protons and π^+ in 158 A GeV $^{208}\text{Pb} + ^{208}\text{Pb}$ and present a detailed analysis of its rapidity dependence at the intermediate centrality where it is greatest.

The present analysis makes use of a subset of the detector systems of the WA98 experiment. This subset consists of the trigger detectors, the Plastic Ball detector, and the tracking spectrometers. The large aperture dipole magnet, Goliath, provided momentum analysis for

the tracking detectors. The data presented were taken during the 1996 SPS run period with 158 A GeV ^{208}Pb beams using a 213 μm thick ^{208}Pb target. The WA98 minimum bias cross section for this run period, with magnetic field on, was $\sigma_{mb} = 6450$ mb.

The trigger detectors consisted of a nitrogen gas Čerenkov counter to provide a fast beam trigger (≤ 30 ps time resolution), beam-halo veto counters, and the MIRAC calorimeter. A beam trigger was defined as a signal in the start counter with no coincident signal in the veto counter (which had a 3 mm diameter circular hole) or in beam halo counters. The MIRAC measures the total transverse energy over the interval $3.2 < \eta < 6.0$ with full azimuthal coverage over the interval $3.7 < \eta < 4.9$. The WA98 minimum bias trigger requires a clean beam trigger with a MIRAC transverse energy which exceeds a low threshold.

The Plastic Ball detector provides full azimuthal coverage in the target fragment region (pseudorapidity $-1.7 < \eta < 0.5$) with 655 detector modules. It provides identification of pions, protons, deuterons, and tritons (π , p, d, and t) with kinetic energies of 50 to 250 MeV by the $\Delta E - E$ method. In addition, stopped π^+ are identified by detection of the delayed e^+ from the decay $\pi^+ \rightarrow \mu^+ + \nu_\mu \rightarrow e^+ + \nu_e + \bar{\nu}_\mu + \nu_\mu$ in the Plastic Ball. For the present analysis the rapidity region $-0.6 < y(\text{proton}) < 0.3$ has been used.

The measurement of identified particles near mid-rapidity was obtained using two large acceptance tracking arms beginning about 3.3 meters downstream of the Goliath magnet. With the normal operation magnetic field setting the first tracking arm was located to the side of negative charge deflection and the second tracking arm to the side of positive charge deflection. The positive charge results are presented here. The momentum resolution of the tracking system may be parameterized as $\Delta p/p \sim 0.97\% + 0.16\% p + 0.023\% p^2$ (p in GeV/ c). The acceptance for protons covered an interval $\Delta y_p \approx 0.3$ which shifted with transverse momentum to provide coverage over the region $1.4 < y_p < 2.4$. Particle identification was obtained by time-of-flight measurement with a resolution of < 90 ps.

We determine the reaction plane as the azimuthal direction, Φ_0 , opposite to \vec{P}_T , the total transverse momentum vector of fragments (p, d, and t) detected in the target rapidity region in the Plastic Ball detector.¹ To check for detector effects, mixed events are created by mixing particles from different events keeping the same multiplicity distribution as in the real events. The mixed events are then analyzed in the same manner as the real events. The laboratory distribution of Φ_0 is nearly uni-

¹Note: the opposite direction is chosen by convention that the projectile fragments define the direction of positive flow.

form, with less than 2% variations. The Φ^{mix} distribution for mixed events is observed to show the same weak variations indicating small detector effects. The data have not been corrected for this effect since the analysis of the mixed events shows a negligible result.

In order to study how well the fragment flow direction is defined, we divide each event randomly into two equal sized subevents and determine a fragment flow direction for each subevent, Φ_a and Φ_b . If the direction of \vec{P}_T is well-defined, the directions determined from each subevent should be strongly correlated [6,19,11]. In Fig. 1, the $\Phi_a - \Phi_b$ correlation is shown for two different centrality bins. As expected, the correlation observed for semi-central events is significantly larger than for very central events. Also shown are the results for mixed events allowing (open squares) or forbidding (open circles) multiple module hits. The former case demonstrates that detector non-uniformities are negligible. In the latter case a weak anti-correlation is observed due to the finite detector granularity and an excluded-module effect. The data have been corrected for this effect using such mixed events.

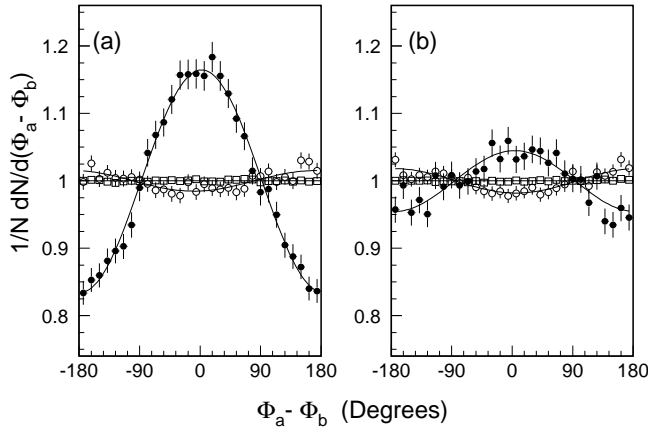


FIG. 1. The distribution of differences between the total transverse momentum directions of two randomly chosen equal size subevents of fragments (p,d,t) in the target rapidity region for a) semi-central ($100 < E_T < 200$ GeV) and b) central ($380 < E_T < 420$ GeV) collisions of 158 A GeV $^{208}\text{Pb} + ^{208}\text{Pb}$. Solid circles are for subevents within the same event. Open points are for subevents constructed from mixed events. Solid curves are fits to guide the eye.

Azimuthal anisotropies of the particle emission are evaluated by means of a Fourier expansion [10,11]. The Fourier coefficients v_n ($n = 1, 2$) are extracted from the azimuthal distribution of identified particles with respect to the reaction plane, Φ_0 , which is determined using all other fragments in the Plastic Ball.

$$\frac{1}{N} \frac{dN}{d(\phi - \Phi_0)} = 1 + 2v_1' \cos(\phi - \Phi_0) + 2v_2' \cos(2(\phi - \Phi_0)), \quad (1)$$

where ϕ is the measured azimuthal angle. The Fourier coefficient v_1' quantifies the directed flow, whereas v_2' quan-

tifies the elliptic flow. The coefficients must be corrected for the event plane resolution as $v_n = v_n' / \langle \cos(n(\Phi_0 - \Phi_r)) \rangle$ where $\Phi_0 - \Phi_r$ is the deviation of the measured reaction plane from the true reaction plane. The event plane resolution may be extracted from the correlation between subevents. For weak correlations one expects $\langle \cos(\Phi_0 - \Phi_r) \rangle \simeq \sqrt{2 \langle \cos(\Phi_a - \Phi_b) \rangle}$. Using the more accurate procedure and interpolation formula of Ref. [11] one obtains $\langle \cos(\Phi_0 - \Phi_r) \rangle = 0.377 \pm 0.018$ for the semi-central ($100 < E_T < 200$ GeV) event selection.

The dependence of the v_1 fit parameter on centrality, as determined by the measured transverse energy (E_T), is shown in Fig. 2. For convenience an impact parameter scale is also shown. The E_T scale has been converted to an impact parameter scale assuming a monotonic relationship between the two quantities, and equating $d\sigma/dE_T$ with $d\sigma/db$. As seen in Fig. 2, the strength of the directed flow of protons increases with centrality and reaches a maximum value for semi-central collisions with $b \approx 8$ fm. It is interesting to note that the strongest flow effect occurs at larger impact parameters than observed at lower incident energy for similar systems (where $b \approx 4$ fm) [4,12]. For comparison, RQMD 2.3 [22] model predictions are shown subjected to the same analysis after applying the Plastic Ball detector acceptance, but using the true reaction plane. RQMD predicts a significantly stronger correlation than observed.

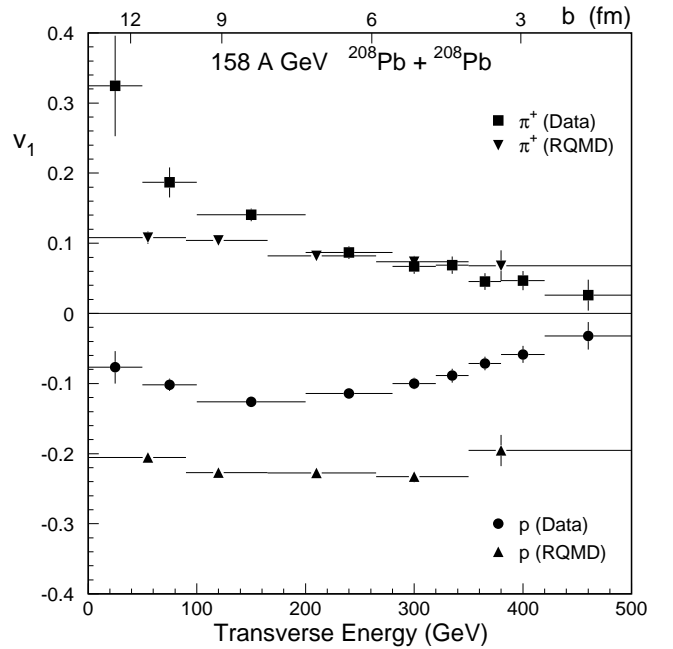


FIG. 2. The centrality dependence of the directed flow coefficient v_1 for protons (circles) and π^+ (squares). Triangles are results from RQMD model calculations. The data have been corrected for the event-plane resolution. The vertical bars indicate the uncertainty of the fit and resolution correction. The horizontal bars indicate the E_T bin intervals (or impact parameter intervals for RQMD).

Also shown in Fig. 2 is the strength of the directed flow of π^+ , identified in the Plastic Ball. A clear anti-correlation, or anti-flow [20], is observed between the fragment and π^+ flow directions. This behaviour has been observed at incident energies from 1 A GeV to SPS energies and has been explained as resulting from preferential absorption of the pions emitted in the target spectator direction [13,14,20,21]. The absorption results in an oppositely directed apparent π^+ flow. The strength of the anti-correlation increases for the most peripheral events, indicating the increasing role of absorption.

A conventional directed flow analysis has been performed [19], in which the average transverse momentum with respect to the reaction plane $\langle p_x \rangle$ is evaluated as a function of rapidity. This is done for semi-central collisions ($100 < E_T < 200$ GeV) where the largest azimuthal asymmetry is observed (see Fig. 2). The distribution $d^3N/dp'_x dp'_y dy$ is constructed for protons and π^+ in the Plastic Ball and in the tracking arm, where the new axis p'_x corresponds to the reaction plane determined event-by-event using all remaining fragments measured in the Plastic Ball (then reflected, $p'_x \rightarrow -p'_x$, to correspond to the projectile fragment direction, according to convention). At each rapidity the average transverse momentum in the reaction plane, $\langle p'_x \rangle$, is calculated from fits to the experimental distributions.

Similar to v_n , the average projected momenta are reduced by $\langle p'_x \rangle = \langle p_x \rangle \cdot \langle \cos(\Phi_0 - \Phi_r) \rangle$. After correction for the event-plane resolution, the $\langle p_x \rangle$ for protons and π^+ are plotted as a function of rapidity in Fig. 3. As expected from Fig. 2, the π^+ show an anti-flow relative to the proton flow. Summing over the Plastic Ball acceptance $\langle p_x \rangle$ values of 8.2 ± 0.7 , -24.9 ± 1.9 , -53.6 ± 4.1 , and -78.4 ± 5.8 MeV/c are obtained for π^+ , p, d, and t, respectively. The observed scaling with fragment mass for p, d, and t indicates emission sources with a common collective motion.

The main sources of systematic error in the present analysis are: detector non-uniformities, contamination in the particle identification, and fit biases in extracting $\langle p_x \rangle$ [23]. The mixed event analysis indicates that systematic errors from detector non-uniformities are less than 2%. The effect of contamination has been estimated by Monte Carlo simulations. The amount of contamination can be estimated from fitting the background underlying the peaks in the Plastic Ball particle identification spectra. For example, the amount of contamination in the proton sample varies from 6% in peripheral events to 26% in central events. The effect of contamination has been estimated in simulation by analyzing events with various amounts and types of contaminated particle distributions compared to pure particle distributions, where the various distributions are taken to have spectra and flow characteristics similar to those measured. These studies indicate a maximum systematic error of 8.5%. The extraction of $\langle p_x \rangle$ is estimated to have an additional

15% uncertainty deduced from observed variations in the results depending on the fit region or method used to fit the $d^3N/dp'_x dp'_y dy$ distribution. These systematic errors have not been included in Figs. 2 or 3.

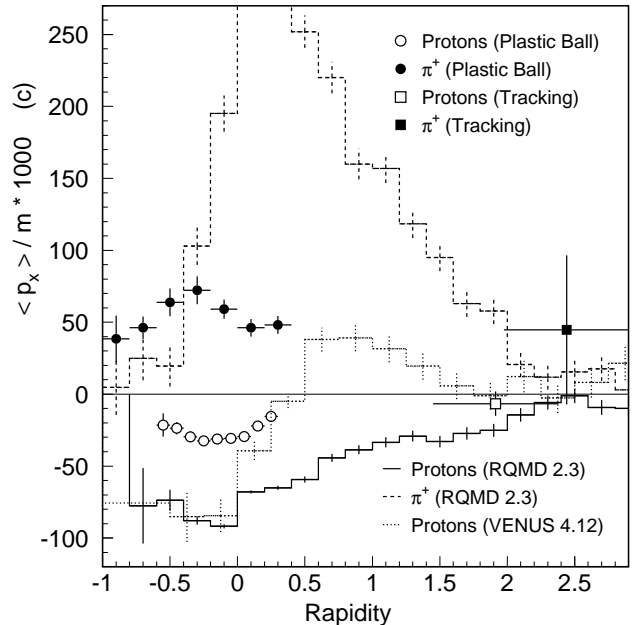


FIG. 3. The average transverse momentum projected onto the reaction-plane for semi-central 158 A GeV $^{208}\text{Pb} + ^{208}\text{Pb}$ collisions (note $y_{cm} = 2.9$). The vertical errors indicate the statistical errors of the fit only. The horizontal bars on the tracking points indicate the width of the rapidity bin. RQMD model calculations ($b=8-10$ fm) and VENUS model calculations ($b=8-10$ fm) are also shown. The VENUS prediction for π^+ (not shown) is similar to that of RQMD.

In Fig. 3 the measured results are compared to RQMD 2.3 [22] and VENUS 4.12 [24] predictions for similar impact parameter range. The RQMD calculation, in cascade mode, overpredicts the observed proton flow by about a factor of three. On the other hand, at AGS energies cascade mode RQMD calculations underpredict the observed directed flow by about a factor of two, but reasonable agreement is obtained when mean field effects are included [13]. At SPS energies mean field effects are expected to be smaller, but would increase the observed disagreement. The VENUS predictions show a similar disagreement in the target rapidity region. The results suggest a significant softness in the nuclear response. The maximum proton $\langle p_x \rangle$ observed is in better agreement with predictions of the Quark Gluon String Model (with rescattering) of Ref. [5] and with a 3-fluid hydrodynamical model calculation [25]. However, these predictions have not been filtered with the experimental acceptance and both calculations predict that the maximum $\langle p_x \rangle$ occurs about one unit forward of the target rapidity. It is interesting to note that VENUS predicts a complicated proton flow behaviour with protons hav-

ing an anti-flow direction (similar to the RQMD pion prediction) near mid-rapidity. However, this prediction disagrees with the results of Ref. [18].

In summary, the directed flow of protons and π^+ has been studied in 158 A GeV $^{208}\text{Pb} + ^{208}\text{Pb}$ collisions. The directed flow is largest for impact parameter ≈ 8 fm, which is considerably more peripheral than observed at lower incident energies. The π^+ directed flow is in the direction opposite to the protons, similar to observations at 11 A GeV energy [13]. The magnitude of the proton directed flow is much less than cascade mode RQMD model predictions, which underpredict the proton flow at AGS energies. It is also much less than VENUS model predictions. The results indicate a soft nuclear response compared to these model predictions at SPS energies.

We express our gratitude to the CERN accelerator division for the excellent performance of the SPS accelerator complex. We gratefully acknowledge the effort of all engineers, technicians, and support staff who have made possible the construction and operation of this experiment.

This work is supported by the German BMBF and DFG, the U.S. DOE, the Swedish NFR and FRN, the Dutch Stichting FOM, the Department of Atomic Energy, the Department of Science and Technology, and the University Grants Commission of the Government of India, the Indo-FRG Exchange Programme, the Stiftung für Deutsch-Polnische Zusammenarbeit, the Grant Agency of the Czech Republic under contract No. 202/95/0217, the PPE division of CERN, the Swiss National Fund, the INTAS under contract INTAS-97-0158, the Grant-in-Aid for Scientific Research (Specially Promoted Research & International Scientific Research) of the Ministry of Education, Science and Culture, JSPS Research Fellowships for Young Scientists and also by the University of Tsukuba Special Research Projects, and ORISE. ORNL is managed by Lockheed Martin Energy Research Corporation under contract DE-AC05-96OR22462 with the U.S. Department of Energy. MIT is supported by the U.S. Department of Energy under the cooperative agreement DE-FC02-94ER40818.

- (1995).
- [8] D.H. Rischke, Nucl. Phys. **A610** (1996) 88c.
 - [9] H. Sorge, Phys. Rev. Lett. **78**, 2309 (1997).
 - [10] S.A. Voloshin and Y. Zhang, Z. Phys. **C70**, 665 (1996).
 - [11] A.M. Poskanzer and S. A. Voloshin, Phys. Rev. **C58**, 1671 (1998).
 - [12] E877 Collaboration, J. Barrette, *et al.*, Phys. Rev. Lett. **73**, 2532 (1994).
 - [13] E877 Collaboration, J. Barrette, *et al.*, Phys. Rev. **C 56**, 3254 (1997).
 - [14] WA80 Collaboration, T.C. Awes, *et al.*, Phys. Lett. **B 381**, 29 (1996).
 - [15] WA93 Collaboration, M.M. Aggarwal, *et al.*, Phys. Lett. **B 403**, 390 (1997).
 - [16] NA49 Collaboration, T. Wienold, *et al.*, Nucl. Phys. **A 610**, 76c (1996).
 - [17] WA98 Collaboration, M. Kurata, *et al.*, p.549 and S. Nishimura, *et al.*, p.258, Physics and Astrophysics of Quark Gluon Plasma, Narosa Publishing House (1998).
 - [18] NA49 Collaboration, H. Appelshäuser, *et al.*, Phys. Rev. Lett. **80**, 4136 (1998).
 - [19] P. Danielewicz and G. Odyniec, Phys. Lett. **157B**, 146 (1985).
 - [20] A. Jahns, *et al.*, Phys. Rev. Lett. **72**, 3463 (1994).
 - [21] A. Kugler, *et al.*, Acta Phys. Pol. **25**, 691 (1994).
 - [22] H. Sorge, Phys. Rev. **C 52**, 3291 (1995).
 - [23] M. Kurata, PhD thesis, University of Tsukuba. H. Schlagheck, PhD thesis, University of Münster.
 - [24] K. Werner, Phys. Rep. **232**, 87 (1993).
 - [25] A. Dumitru, *et al.*, Heavy Ion Phys. **5**, 357 (1997).

-
- [1] H.Å. Gustafsson, *et al.*, Phys. Rev. Lett. **52**, 1590 (1984).
 - [2] H. Stöcker and W. Greiner, Phys. Rep. **137**, 277 (1986).
 - [3] J. Aichelin, *et al.*, Phys. Rev. Lett. **58**, 1926 (1987).
 - [4] See for example, W. Reisdorf and H.G. Ritter, Ann. Rev. Nucl. Part. Sci. **47**, 663 (1997).
 - [5] N.S. Amelin, *et al.*, Phys. Rev. Lett. **67**, 1523 (1991).
 - [6] J.-Y. Ollitrault, Phys. Rev. **D 46**, 229 (1992); J.-Y. Ollitrault, Phys. Rev. **D 48**, 1132 (1993).
 - [7] C.M. Hung and E.V. Shuryak, Phys. Rev. Lett. **75**, 4003